

**CHARACTERISATION OF ERBIUM-DOPED FIBRE AMPLIFIERS**  
**R.I. LAMING**  
**OPTOELECTRONICS RESEARCH CENTRE, THE UNIVERSITY, SOUTHAMPTON,**  
**S09 5NH, UNITED KINGDOM**

**ABSTRACT**

Experimental techniques necessary to characterise, and thus to optimise the design of both erbium-doped fibres and erbium fibre amplifiers are described.

**I INTRODUCTION**

Erbium-doped fibre amplifiers (EDFA) have recently attracted considerable attention in the field of optical fibre communications since they conveniently operate in the preferred telecommunications spectral-window located around  $1.55\mu\text{m}^{1-7}$ . It has been demonstrated that an EDFA can be optically pumped at a number of wavelengths ( $514\text{nm}^2$ ,  $532\text{nm}^3$ ,  $665\text{nm}^1$ ,  $800\text{nm}^8$ ,  $980\text{nm}^{3,4,9}$  and  $1.49\mu\text{m}^{5,10,11}$ ), with high-gain<sup>10</sup>, efficient diode-pumped operation being demonstrated at pump wavelengths of  $980\text{nm}^{4,9}$  and  $1.49\mu\text{m}^{5,10}$ . In addition the EDFA has been shown to exhibit polarisation-insensitive gain, low crosstalk<sup>12-16</sup> between signals at different wavelengths, a high saturation output power and noise figure close to the quantum limit<sup>17-20</sup>. A variety of host glasses and fibre designs are being investigated with a view to optimising amplifier characteristics such as pump efficiency or spectral bandwidth<sup>21,22</sup>.

Measurement of a wide range of parameters of erbium-doped fibre are described. From these amplifier performance may be inferred. Subsequent techniques for detailed analysis of EDFA performance are presented.

**II FIBRE CHARACTERISATION**

**A. Spectral Absorption.** Measurement of spectral loss in  $\text{Er}^{3+}$ -doped fibres is complicated by the intense absorption caused by electronic transitions in the ions, combined with losses approaching those of telecommunications fibres away from the bands<sup>23-25</sup>. A typical spectrum is shown in Figure 1 for a fibre doped with around 300ppm  $\text{Er}^{3+}$  ( $\lambda_c \approx 1250\text{nm}$ ). Intense bands (60,000dB/km) are recorded adjacent to a baseline loss of 7dB/km. A multiple cutback technique<sup>23</sup> of high spectral resolution is employed to determine loss peaks. For very short lengths (<5cm) cladding modes are removed by the photon bucket method<sup>26</sup>. Average dopant concentrations can be estimated from attenuation plots if the overlap of the optical field with the fibre core is considered.

**B. Excited-State Absorption (ESA).** ESA is the absorption by an already excited ion of additional energy, so reducing amplifier efficiency by wasting signal or pump photons<sup>27-29</sup>. Signal ESA is negligible in  $\text{Er}^{3+}$ -doped  $\text{SiO}_2$ -based fibre<sup>29</sup> but pump ESA limits choice of pump sources, and may be quantified by using the configuration<sup>27</sup> of Figure 2. Chopped white light is launched into a short section of doped fibre. The throughput is spectrally analysed with the fibre unpumped, and in the presence of counter-propagating pump light. Thus the difference between the ESA and ground-state absorption (GSA) is obtained. A cutback measurement then allows the unpumped loss i.e. GSA to be extracted.

A typical ESA spectrum is shown in Figure 3 for an  $\text{Er}^{3+}$ -doped  $\text{Al}_2\text{O}_3/\text{SiO}_2$  core fibre. It may be seen that ESA extends across the potentially diode pumpable band around 807nm indicating that much of the pump energy will be dissipated non-radiatively. However no ESA is observed on the 980nm transition, emphasising the importance of ESA measurements for identification of ideal pump bands. The ratio of ESA and GSA cross-sections,  $\sigma_{\text{ESA}}/\sigma_{\text{GSA}}$  at any wavelength indicates the degree of pump ESA and is listed in Table 1 for several host glasses.

**C. Fluorescence Measurements.** Emission spectra and decay time data allow the estimation of emission cross-section for the fibre under test<sup>24,30-34</sup>. Hence information on the gain profile and eventual amplifier efficiency is obtained<sup>35</sup>.

**C1. Spectral Characteristics.** A typical fluorescence measurement configuration is shown in Figure 4. In the three-level  $\text{Er}^{3+}$  system both pump wavelength and fibre length are important. In-band pumping (1490nm) is avoided since residual pump energy will mask the weak fluorescence. Further, both amplified spontaneous emission (ASE) and reabsorption distorts the output<sup>34</sup>, however their effect is reduced by monitoring side-light emission or by employing a

short length of fibre such that stimulated emission and absorption are negligible (<0.1dB loss). Fluorescence spectra for two Er<sup>3+</sup>-doped fibres of different core glasses are shown in Figure 5, where the host is seen to alter the spectral profile. Identification of the Stark splitting responsible for the irregular profile can be obtained from fluorescence line-narrowing data<sup>36</sup>. Note also the broad bandwidth (>200nm) of the emission, thus the measurement system must be carefully calibrated.

**C2. Time-Dependent Characteristics.** To determine emission decay-time characteristics, the Er<sup>3+</sup>-doped fibre is excited by a pulsed source and the exponential decay in fluorescence emission monitored directly. Short sample lengths are employed to ensure that the stimulated emission rate due to ASE is significantly weaker than the spontaneous rate. Alternatively, if sufficient signal is available, side-scattered light should be measured.

Typical Er<sup>3+</sup>-doped fibres exhibit truly exponential emission decay times,  $\tau_{fl}$ , of 10-12ms, dependent on host glass. Non-exponential decay is evidence of detrimental effects such as concentration quenching or co-operative upconversion<sup>29</sup>.

Short initial decay components (<10 $\mu$ s) have been observed in clustered fibres<sup>29</sup>. Ideally these should be resolved by pumping with a pulsed source (<1 $\mu$ s), directly into the metastable manifold. This is because long-lived (5 $\mu$ s) non-radiative decay from higher energy bands to the metastable level will mask these components for other pump wavelengths.

**D. Dopant Distribution.** Since erbium is a three-level system, improvements in amplifier performance can be obtained by localising the dopant in regions of high pump intensity<sup>4,37,38</sup>. This has the effect of maximising the population inversion for a given pump power and thus minimises re-absorption due to unexcited ions. Typical amplifiers, pumped at either 980nm or 1.49 $\mu$ m, are designed such that only the fundamental pump and signal modes propagate and thus it can be desirable to localise the dopant in the centre of the fibre core.

A quantitative measure of the dopant concentration and distribution is obtained using either dispersive electron probe microanalysis (EPMA)<sup>38</sup>, or secondary ion mass spectroscopy (SIMS). For both measurements, the dopant distribution is determined from preform samples or large core fibres owing to the limited resolution (typically 2 $\mu$ m) of the measurement systems (see Figure 6). Knowledge of the dopant distribution may then be used to modify the fabrication process and hence optimise the radial dopant profile for device applications<sup>38</sup>.

**E. Saturation Measurements.** A qualitative measure of the dopant distribution in the fibre can be obtained by measuring the pump threshold,  $P_{TH}$ , the power required to bleach an infinitesimally-short section of fibre. For a given fibre NA and cutoff wavelength, a lower value of  $P_{TH}$  implies a higher degree of dopant confinement and a more efficient overlap,  $\eta_p$ , between the pump field and dopant<sup>35</sup>.

$P_{TH}$  is determined experimentally by monitoring side-scattered fluorescence from a short section of fibre as a function of pump power; the pump wavelengths being chosen to be free from ESA (e.g. 980nm). Figure 7 shows a typical measurement.  $P_{TH}$  is defined as the pump power at which the fluorescence attains half its maximum value and can be expressed:

$$P_{TH} = \frac{h\nu_p}{\sigma_p \tau_{fl}} \frac{a}{\eta_p}$$

where  $h\nu_p$  is the pump photon energy,  $a$  the core area and  $\sigma_p$  the pump absorption cross-section. For fibres of similar core composition, NA and  $\lambda_{cutoff}$  such that  $\sigma_p$ ,  $\tau_{fl}$  and  $a$  are constant,  $P_{TH}$  gives a qualitative measure of the dopant confinement  $\eta_p$ . Generally, the higher the value of  $\eta_p$  the better the fibre. Alternatively, if the fibre parameters and dopant distribution are known accurately, the overlap parameter  $\eta_p$  can be evaluated numerically and thus the absorption cross-section,  $\sigma_p$  determined from such a measurement<sup>31</sup>.

### III AMPLIFIER CHARACTERISATION

**A. Gain Characterisation.** A typical configuration for the measurement of amplifier gain is shown in Figure 8. The input signal from a DFB laser, wavelength selected to match the peak gain of the fibre under test, is combined with the pump light via a dichroic coupler and input to the amplifier fibre. At the output the residual pump light is filtered. Direct modulation of the input signal at -20kHz and monitoring of the amplified output with lock-in techniques allows the output signal to be separated from the unmodulated ASE<sup>12</sup>. Optical feedback is prevented by angle polishing the fibre ends.

The gain of an EDFA depends on the input signal, pump power and fibre length. Thus it is impossible to design an amplifier which is optimised for all operating conditions. For example, Figure 9 shows the dependence of amplifier output on fibre length for a range of input signals and a constant pump power of 6.2mW. It is clear that the optimum length decreases with increasing input signal. In addition, the optimum length is known to increase with pump power<sup>2</sup>. Thus the intended operating conditions must be considered when characterising an EDFA.

Once the optimum fibre length has been determined the dependence of amplifier gain on input power can be established. Figure 10 shows such curves where the amplifier length is optimised for small signal gain<sup>4</sup>. It is noted that, for these high gain amplifiers, gain compression occurs at low (-35dBm) input signal powers.

The gain per unit pump power<sup>3</sup> (dB/mW) is a useful figure of merit for EDFA's, and can be determined from the previous curves. Alternatively, small signal amplifier gain is measured as a function of pump power for a given fibre length (typically equivalent to 50dB signal absorption) and the maximum of their ratio quoted. Care must be taken in interpreting these figures since they depend on fibre parameters such as NA and  $\lambda_{\text{cutoff}}$ .

**B. Spectral Gain Bandwidth.** The gain bandwidth is an important parameter for system design, particularly when several amplifiers are concatenated. However, the EDFA bandwidth is influenced by the method of determination.

The small-signal gain bandwidth is easily determined using either a broadband, low-power ELED as the input and monochromator at the output<sup>22</sup>, or via a wavelength-scanned tunable laser diode with output attenuated to give a small-signal input (<100nW). However if the large signal spectral gain is determined with a single, large (-100 $\mu$ W) tunable input, a relatively flat gain spectrum is obtained. This is due to the near homogeneous line-broadening in erbium which allows near constant power extraction and thus gain, for a wide range of input signals<sup>39</sup>. This result would be significantly different if several lasers covering the gain spectrum were employed simultaneously<sup>40</sup>.

**C. Homogeneous Linewidth.** Knowledge of the homogeneous and inhomogeneous components in the spectral gain profile allows optimisation of the amplifier saturation characteristics and hence the determination of glass host most suited to multichannel operation. Two methods have been employed. First, cross-saturation of the gain from two closely-spaced (-0.75nm) signal wavelengths is monitored at room temperature<sup>12</sup>. Alternatively, spectral gain hole burning at reduced temperatures is measured from which the room temperature homogeneous and inhomogeneous linewidths are inferred<sup>41</sup>.

**D. Phase Noise.** Spectral broadening due to phase noise introduced by chained erbium-doped-fibre amplifiers may limit the number of amplifiers which can be concatenated in an optical link. Spectral broadening in an EDFA has been measured using a novel Mach-Zehnder interferometer containing the amplifier in one arm<sup>42</sup>. Provided that the optical paths in the interferometer are matched in length such that the propagation time difference between the light passing through the two arms is much less than the coherence time of the DFB laser source, the technique effectively deconvolves the DFB laser spectrum from the amplifier spectral broadening. The interferometer thus provides an output which consists solely of the amplifier spectral broadening response to a zero-linewidth input spectrum.

A typical measured power spectral density (PSD) is shown in Figure 11. This shows an

approximately Lorentzian lineshape, with a half-power spectral width of less than 20kHz and indicates the signal broadening.

**E. Noise Measurements.** The output from an optical fibre amplifier is a combination of amplified signal and broad-spectrum ASE. If the input signal is coherent, its noise contribution is the usual shot noise associated with the amplified signal level. There is also a shot noise associated with the level of the ASE. Additional noise terms are introduced by the mixing on the detector of the amplified signal and spectral components of the ASE to give signal-spontaneous (sig-sp) beat noise and spontaneous-spontaneous (sp-sp) beat noise<sup>43</sup>.

The ASE spectral density of a three-level system and thus the power spectral density (PSD) of both the sig-sp and sp-sp beat noises are a direct function of the amplifier inversion parameter,  $\mu$ .  $\mu$  is defined by  $N_2/(N_2-N_1)$ , where  $N_1$  and  $N_2$  are the population densities of the ground and metastable states respectively. Thus the EDFA noise characteristics depend on pump power and wavelength as well as fibre parameters such as NA and  $\lambda_{\text{cutoff}}$ . The PSD of the sig-sp beat noise is proportional to input signal and independent of optical bandwidth, conversely, sp-sp beat-noise is independent of input signal but a direct function of optical bandwidth. Thus for weak input signals and/or a large optical bandwidth, the noise is dominated by sp-sp beat-noise whereas for higher input signals and/or reduced optical bandwidth, sig-sp beat-noise dominates. In the latter the amplifier NF reduces to  $2\mu$ , the minimum NF possible being 3dB<sup>17</sup>.

Several techniques have been employed to characterise amplifier noise<sup>18-20</sup> of which RF spectral analysis of the detected amplifier output is the most widely used<sup>18,20</sup>. The PSD is recorded for a wide range of input signals allowing identification of the contribution from individual noise components. Thus the amplifier inversion parameter  $\mu$  and NF are determined<sup>18</sup>. Alternative techniques include heterodyne measurement<sup>44</sup> of the NF or direct optical measurement of the ASE spectral density<sup>20</sup>.

#### IV CONCLUSIONS

Key experimental techniques for the characterisation and optimisation of erbium-doped fibres and EDFAs have been outlined.

#### V ACKNOWLEDGEMENTS

The collaboration of J.E. Townsend, P.R. Morkel, W.L. Barnes, G.J. Cowle, N.J. Payne and D.N. Payne is greatly appreciated. Thanks are also due to Pirelli General plc for the provision of a Senior Research Fellowship.

#### VI REFERENCES

1. R.J. Mears et al., *Elect. Lett.*, Vol. 23, pp. 1026-1028, 1987.
2. E. Desurvire et al., *Opt. Lett.*, Vol. 12, pp. 888-890, 1987.
3. R.I. Laming et al., *Elect. Lett.*, Vol. 25, pp. 12-14, 1989.
4. R.S. Vodhanel et al., *Elect. Lett.*, Vol. 25, pp. 1386-1387, 1989.
5. M. Nakazawa et al., *Appl. Phys. Lett.*, Vol. 54, pp. 295-297, 1989.
6. N. Edagawa et al., *Proc. ECOC*, Paper PDA-8, Gothenburg, 1989.
7. S. Saito et al., *Proc. OFC*, Paper PD2, San Francisco, 1990.
8. M. Nakazawa et al., *Elect. Lett.*, Vol. 26, pp. 548-549, 1990.
9. M. Yamada et al., *IEEE Photonics Tech. Lett.*, Vol. 1, pp. 422-424, 1989.
10. M. Nakazawa et al., *Elect. Lett.*, Vol. 25, pp. 1656-1657, 1989.
11. E. Desurvire et al., *Opt. Lett.*, Vol. 14, pp. 1266-1268, 1989.
12. R.I. Laming et al., *Elect. Lett.*, Vol. 25, pp. 455-456, 1989.
13. K. Inoue et al., *Elect. Lett.*, Vol. 25, pp. 594-595, 1989.
14. M.J. Pettitt et al., *Elect. Lett.*, Vol. 25, pp. 416-417, 1989.
15. C.R. Giles et al., *Opt. Lett.*, Vol. 14, pp. 880-882, 1989.
16. W.I. Way et al., *Proc. IOOC*, Paper 20PDA-10, Kobe, Japan, 1989.
17. R. Olshansky, *Elect. Lett.*, Vol. 24, pp. 1363-1365, 1988.
18. R.I. Laming & D.N. Payne, "Noise characteristics of erbium-doped fibre amplifier pumped at 980nm", to be published in *IEEE Photonics Tech. Letts.*
19. M.J. Pettitt et al., *Elect. Lett.*, Vol. 25, pp. 273-275, 1989.

20. C.R. Giles et al., IEEE Photonics Tech. Lett., Vol. 11, pp. 367-369, 1989.
21. C.G. Atkins et al., Elect. Lett., Vol. 25, pp. 910-911, 1989.
22. M. Tachibana et al., "Gain-shaped erbium-doped fibre amplifier (EDFA) with broad spectral bandwidth", Proc. Topical Meeting on Optical Amplifiers & their Applications, Monterey, California, 6-8 August 1990.
23. S.B. Poole et al., J. Lightwave Tech., Vol. 4, pp. 870-876, 1986.
24. B.J. Ainslie et al., J. Lightwave Tech., Vol. 16, pp. 287-293, 1988.
25. S.P. Craig-Ryan et al., Elect. Lett., Vol. 26, pp. 185-186, 1990.
26. W.C. Young, in Tech. Digest, Symp. Opt. Fib. Meas., Boulder, Colorado, 1986.
27. R.I. Laming et al., Opt. Lett., Vol. 13, pp. 1084, 1988.
28. C.G. Atkins et al., Opt. Comms., Vol. 73, pp. 217-222, 1989.
29. R. Wyatt, Proc. SPIE Fibre Laser Sources & Amplifiers, Vol. 1171, pp. 54-64, 1989.
30. W.L. Barnes et al., Proc. CLEO, Paper JTUa3, Anaheim, California, 1990.
31. W.L. Barnes et al., "Absorption and emission cross-section of  $Er^{3+}$ -doped silica fibres", Submitted to IEEE J. Quantum Electron. April 1990.
32. J.N. Sandoe et al., J. Phys. D: Appl. Phys., Vol. 5, pp. 1788-1799, 1972.
33. W.J. Miniscalco et al. Proc. SPIE Fibre Laser Sources & Amplifiers, Vol. 1171, pp. 92-102, 1989.
34. E. Desurvire et al., J. Lightwave Tech., Vol. 7, pp. 835-845, 1989.
35. P.R. Morkel et al., Opt. Lett., pp. 1062-1064, 1989.
36. S. Zemon, Proc. SPIE Fibre Laser Sources & Amplifiers, Vol. 1171, pp. 219-236, 1989.
37. J.R. Armitage, Appl. Opt., Vol. 27, pp. 4831-4835, 1988.
38. B.J. Ainslie et al., Proc. ECOC, Vol. IEE 292, Pt II, pp. 62-65, Brighton, 1988.
39. R.I. Laming et al., "Highly-saturated erbium-doped-fibre power amplifiers", Proc. Topical Meeting on Optical Amplifiers & their Applications, Monterey, California, 6-8 August 1990.
40. W.I. Way, Proc. OFC, Paper PD21, San Francisco, 1990.
41. E. Desurvire et al., Proc. CLEO, Paper CFD2, Anaheim, California, 1990.
42. G.J. Cowle et al., Elect. Lett., Vol. 26, pp. 424-425, 1990.
43. T. Mukai et al., IEEE Trans. Microwave Theory & Tech., Vol. MTT-30, p. 1548, 1982.
44. R.S. Vodhanel et al., Proc. OFC, Paper WL4, San Francisco, 1990.

Fibre type Wavelength (nm)	GeO <sub>2</sub>	GeO <sub>2</sub> /P <sub>2</sub> O <sub>5</sub>	Al <sub>2</sub> O <sub>3</sub>
488	2.9	1.86	1.74
514.5	0.95	0.55	0.5
655	0.28	0.13	0.14
810	2.0	1.0	1.0
980			0

Table 1 Ratio of excited-state and ground-state cross-sections  $\sigma_{ESA}/\sigma_{GND}$  as a function of wavelength.

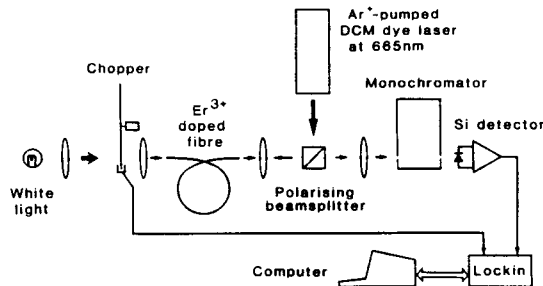


Figure 2 Experimental configuration for the measurement of pump ESA<sup>27</sup>

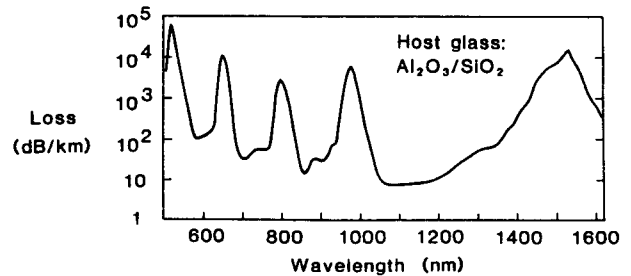


Figure 1 Spectral attenuation of fibre containing around 300ppm  $Er^{3+}$

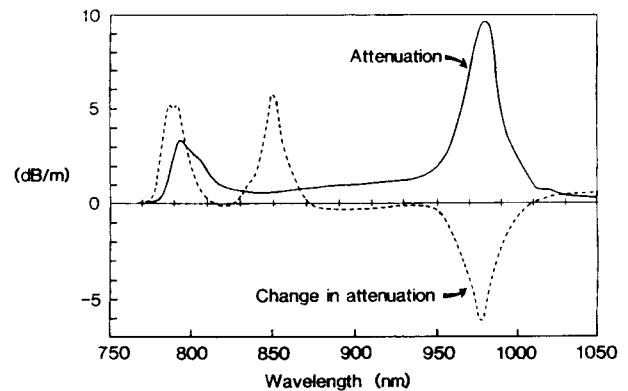


Figure 3 Spectral characteristics of pump ESA in an  $Er^{3+}$ -doped fibre with an  $Al_2O_3$ - $SiO_2$  core<sup>27</sup>

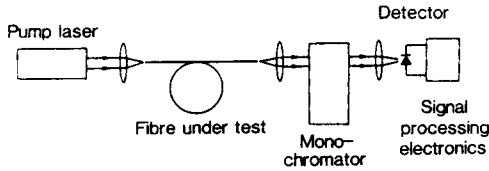


Figure 4 Experimental configuration for measurement of fluorescence<sup>23</sup>

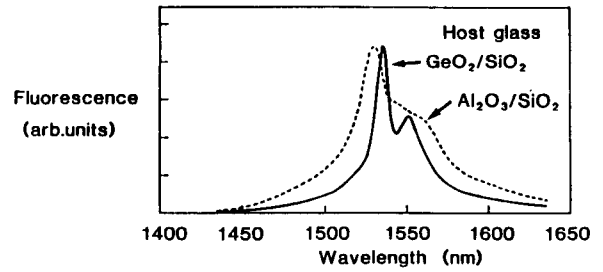


Figure 5 Fluorescence spectra

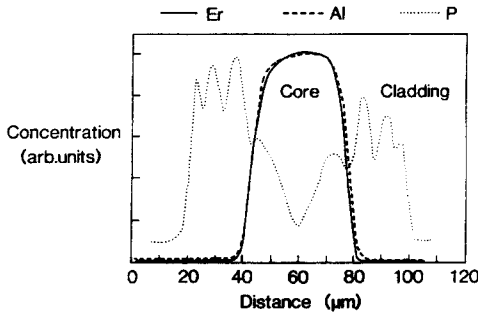


Figure 6 A typical elemental distribution of  $Er^{3+}$ , Al and P across an  $Er^{3+}$ -doped  $Al_2O_3$ - $P_2O_5$ - $SiO_2$  fibre core<sup>38</sup>

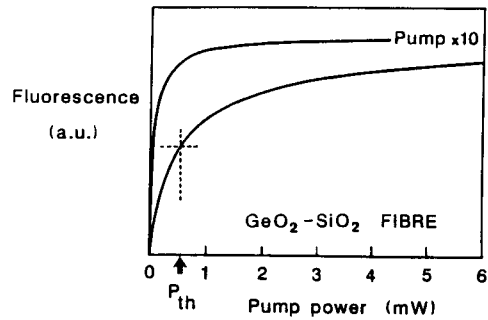


Figure 7 Typical saturation measurement showing the dependence of side-scattered fluorescence on pump power and determination of  $P_{TH}$

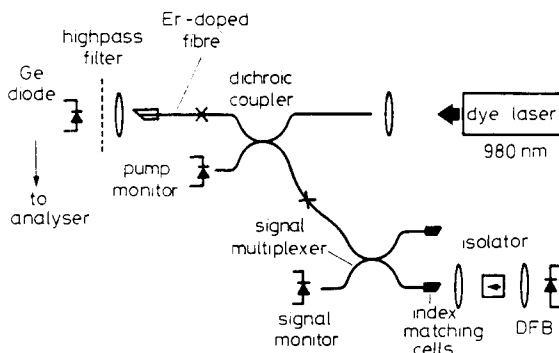


Figure 8 Typical configuration for the measurement of amplifier gain<sup>12</sup>

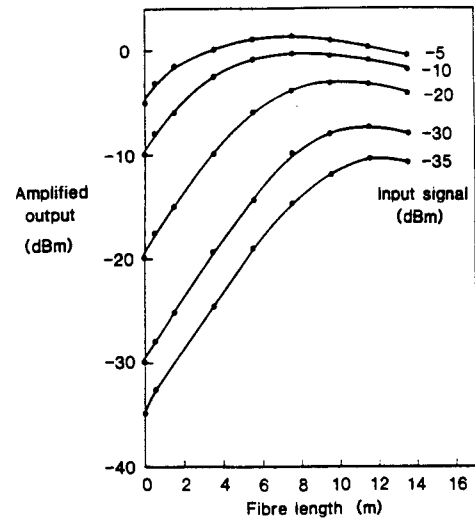


Figure 9 Dependence of amplifier output on fibre length. (Germanosilicate erbium-doped fibre,  $NA \approx 0.2$ ,  $\lambda_{cutoff} \approx 955nm$ , pump power = 6.2mW)

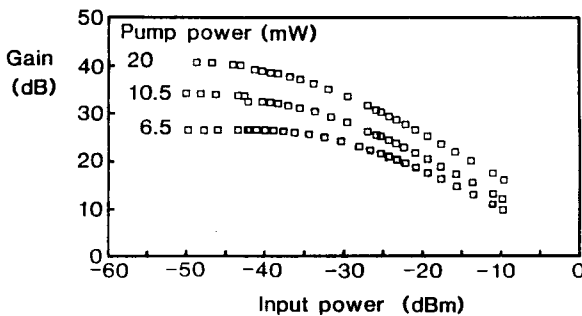


Figure 10 Dependence of amplifier gain on input power<sup>4</sup>. (Germanosilicate erbium-doped fibre,  $NA \approx 0.2$ ,  $\lambda_{cutoff} \approx 955nm$ , pump power = 6.2mW)

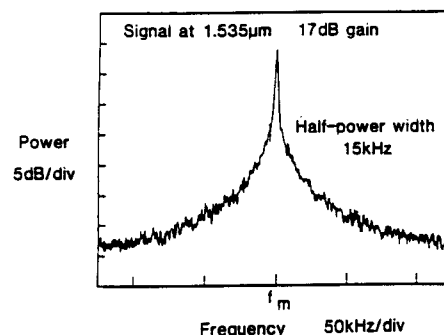


Figure 11 Measured spectral broadening induced by phase noise in an EDFA